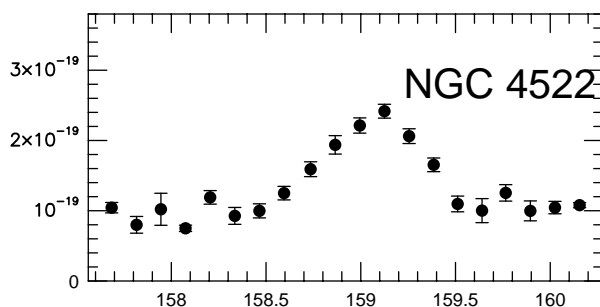
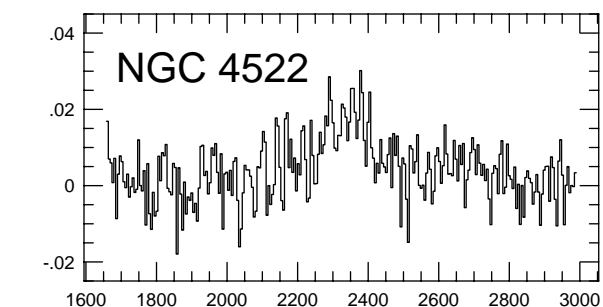
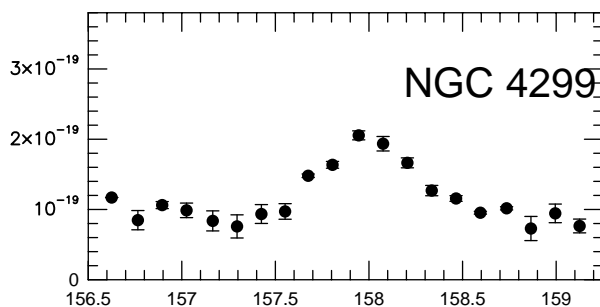
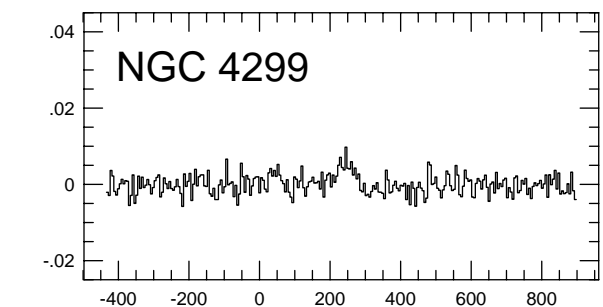
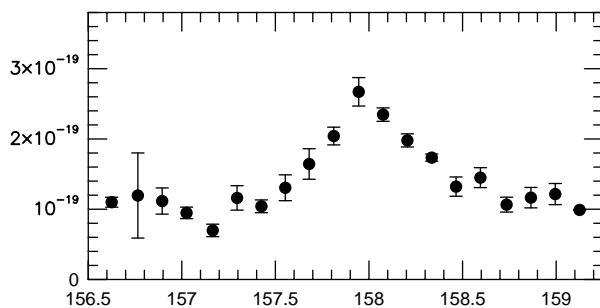
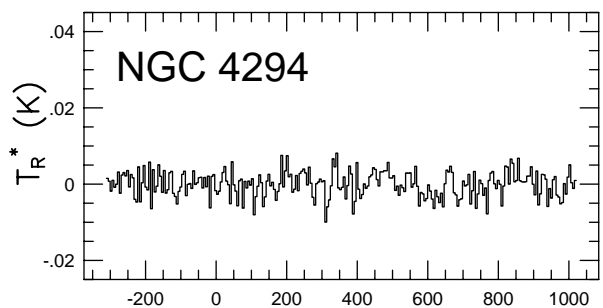
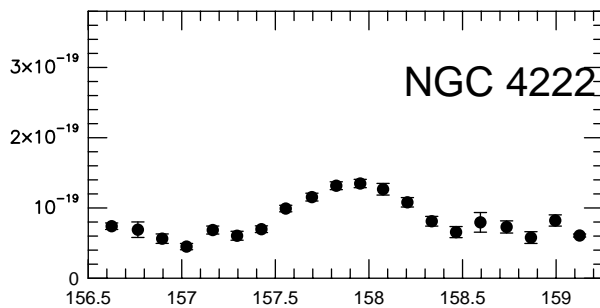
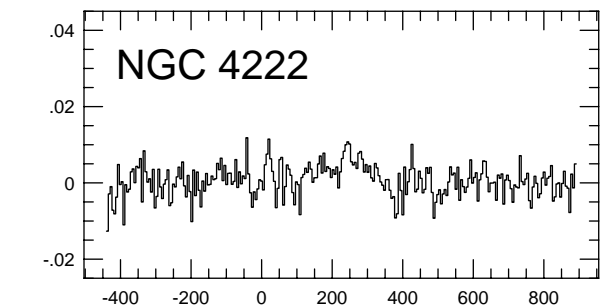
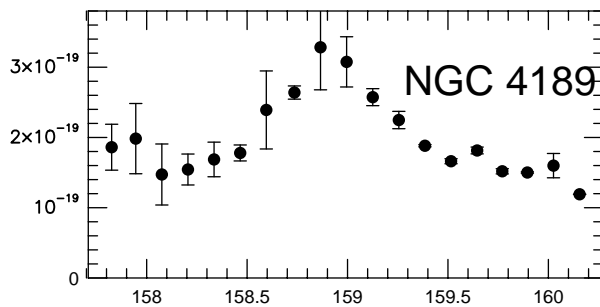
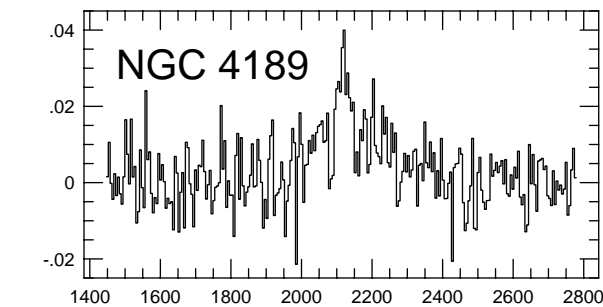


CO (1 - 0)

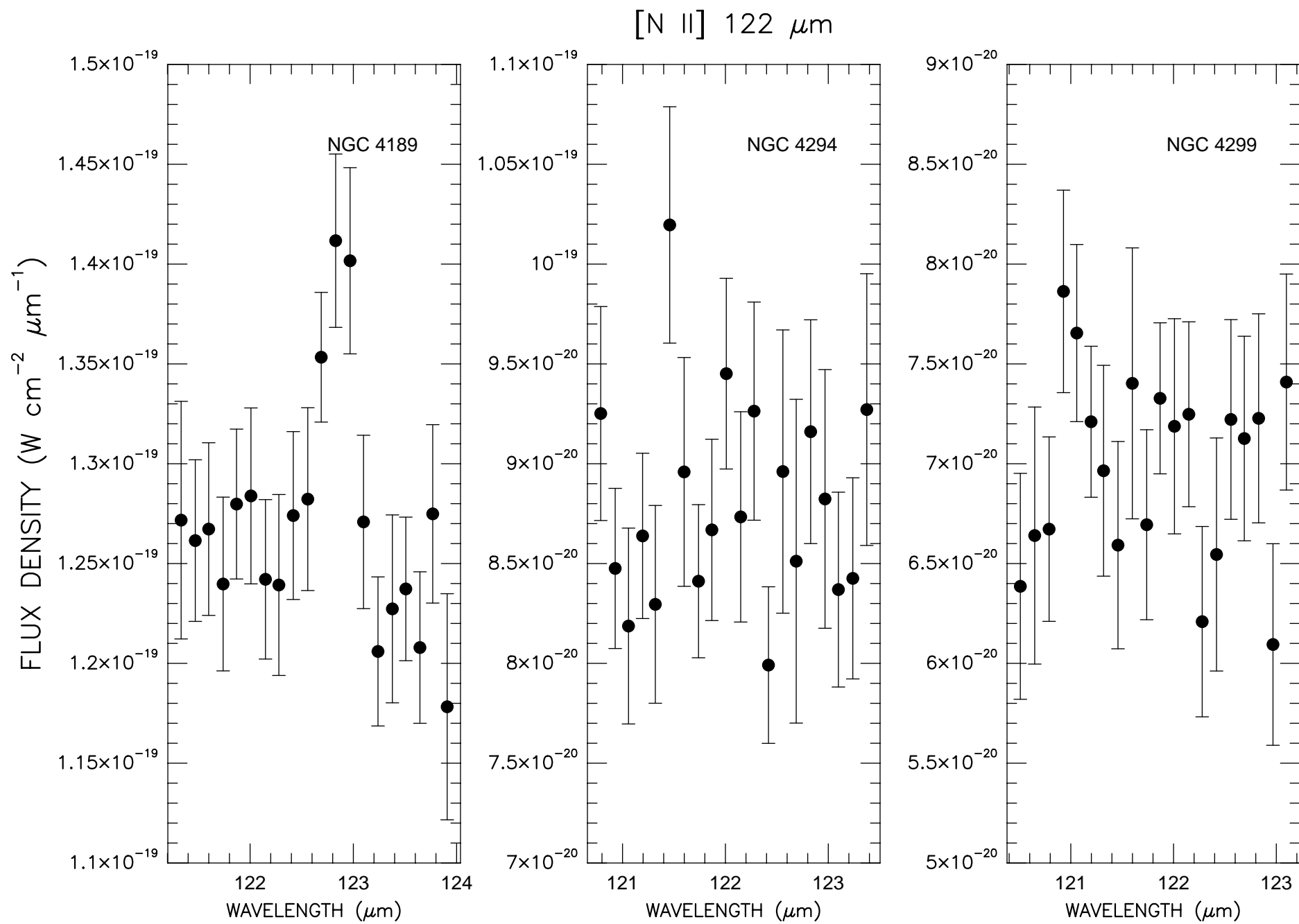
[C II] 158 μm



VELOCITY (km/s)

WAVELENGTH (μm)

FLUX DENSITY ($\text{W cm}^{-2} \mu\text{m}^{-1}$)



Interstellar Gas
in
Low Mass Virgo Cluster Spiral Galaxies¹

Beverly J. Smith

IPAC/Caltech, MS 100-22, Pasadena CA 91125

and

Suzanne C. Madden

Centre d'Etudes de Saclay, Service d'Astrophysique, Ormes des Merisiers, 91191

Gif-Sur-Yvette Cedex, France

Received _____; accepted _____

¹Based on observations made with ISO, an ESA project with instruments funded by ESA Member States and with the participation of ISAS and NASA.

ABSTRACT

We have measured the strengths of the [C II] 158 μm , [N II] 122 μm , and CO (1 – 0) lines from five low blue luminosity spiral galaxies in the Virgo Cluster, using the Infrared Space Observatory and the NRAO 12m millimeter telescope. Two of the five galaxies have high L([C II])/L(CO) and L(FIR)/L(CO) ratios compared to higher mass spirals. These two galaxies, NGC 4294 and NGC 4299, have L([C II])/L(CO) ratios of $\geq 14,300$ and 15,600, respectively, which are similar to values found in dwarf irregular galaxies. This is the first time that such enhanced L([C II])/L(CO) ratios have been found in spiral galaxies. This result may be due to low abundances of dust and heavy elements, which can cause the CO (1 – 0) measurements to underestimate the molecular gas content. Another possibility is that radiation from diffuse HI clouds may dominate the [C II] emission from these galaxies. Less than a third of the observed [C II] emission arises from HII regions.

Subject headings: Galaxies: Clusters (Virgo)

1. Introduction

The 2.6mm CO (1 - 0) line is commonly used as a measure of the mass of interstellar molecular hydrogen in external galaxies (e.g., Young 1990; Young & Scoville 1991). In these studies, the CO intensity is generally assumed to be proportional to the H₂ column density, with a constant of proportionality equal to that found for Galactic clouds. Recent theoretical and observational evidence, however, suggests that this ratio may vary significantly from galaxy to galaxy and within galaxies, as a function of the ambient radiation field, the metal abundance, and the dust extinction. In particular, low abundances of C and O and a low dust column density may result in deeper penetration of ultraviolet photons, decreasing the size of the CO-emitting region within a molecular cloud, while H₂ remains relatively self-shielded. This can result in large volumes of molecular clouds which are not sampled by CO observations (Maloney & Black 1988; Maloney 1990; Maloney & Wolfire 1996). In dwarf irregular galaxies, the CO intensity is generally faint relative to the star formation rate (Combes 1986; Tacconi & Young 1987), perhaps due to this effect rather than to a particularly low H₂ content. CO studies of individual clouds and cloud complexes in dwarf irregular galaxies are consistent with this scenario; the virial masses implied by the line widths are often higher than the H₂ masses indicated by the CO luminosities and the standard I_{CO}/N_{H_2} conversion factor (e.g., Dettmar & Heithausen 1989; Rubio et al. 1991; Wilson & Reid 1992). These investigations suggest that I_{CO}/N_{H_2} is correlated with metallicity, but with significant scatter (Ohta et al. 1993).

Other evidence for a lower I_{CO}/N_{H_2} conversion factor in irregular galaxies compared to the Milky Way is the detection of strong [C II] 158 μ m emission relative to the CO (1 - 0) intensity (Mochizuki et al. 1994; Poglitsch et al. 1995; Israel et al. 1996; Madden et al. 1997), compared to the $L([C II])/L(CO)$ ratio for Galactic star forming regions and the central regions of high mass spiral galaxies (Crawford et al. 1985; Stacey et al.

1991). This C^+ line is an important interstellar cooling line, and in regions of on-going star formation it originates mainly from warm ($T \sim 300K$) dense ($10^2 - 10^4 \text{ cm}^{-3}$) gas in photodissociation regions (PDRs) which form the boundaries between HII regions and molecular clouds (Stacey et al. 1991). In the inner regions of high mass galaxies, the observed $L([C \text{ II}])/L(CO)$ and $L([C \text{ II}])/L(FIR)$ ratios (Stacey et al. 1991) agree with those predicted by theoretical studies of PDRs in gas with solar abundances (Tielens & Hollenbach 1985; Wolfire, Hollenbach, & Tielens 1989). For dwarf irregular galaxies, however, the $L([C \text{ II}])/L(CO)$ ratios do not fit these models (Mochizuki et al. 1994; Poglitsch et al. 1995; Israel et al. 1996; Madden et al. 1997), probably because of the low metallicities of these systems. In gas with low abundances and dust content, UV radiation penetrates more deeply into a molecular cloud, causing a larger C^+ region relative to the CO core, and therefore elevated global $L([C \text{ II}])/L(CO)$ ratios (Maloney 1990; Maloney & Wolfire 1996). It is in this C^+ emitting region that H_2 may be present and unaccounted for by CO observations.

If decreased I_{CO}/N_{H_2} ratios are common in low metallicity systems, then one would expect to find them not only in dwarf irregulars, but also in low mass spiral galaxies, since metallicity appears to be correlated with galaxian mass (Pagel & Edmund 1981; Garnett & Shields 1987; Vila-Costas & Edmunds 1992). A good sample to search for this effect is the low mass Virgo Cluster spirals studied by Kenney & Young (1988). These galaxies have high star formation rates, as measured by their far-infrared and $H\alpha$ luminosities, relative to their CO luminosities, compared to high mass Virgo galaxies. Kenney & Young (1988) suggest that the total gas mass, rather than the molecular gas alone, is important in determining the rate of star formation. An alternative explanation is that the amount of molecular gas is underestimated in the low mass spirals by the CO (1 – 0) line (Kenney & Young 1988, 1989).

To investigate the physical conditions of the interstellar medium in these galaxies and to compare with dwarf irregulars and high mass spirals, we have used the Long Wavelength Spectrometer (LWS) (Clegg et al. 1996) on the Infrared Space Observatory (ISO) (Kessler et al. 1996) to measure the [C II] 158 μm emission from five of the low mass Kenney & Young (1988) Virgo spiral galaxies. To distinguish between [C II] radiation from neutral and ionized gas, we have also observed the [N II] 122 μm line, which originates only in HII regions. Several of these galaxies were undetected in CO (1 – 0) in the Kenney & Young (1988) survey. We have therefore also used the National Radio Astronomy Observatory (NRAO²) 12m telescope to make more sensitive measurements of this line. These results are compared with the IRAS far-infrared fluxes and published H α and HI fluxes, along with results for other galaxies and theoretical models of C⁺ emission.

The sample galaxies are listed in Table 1, along with their positions, types, total blue magnitudes, sizes, and velocities. In Table 2, we provide total far-infrared flux densities from IRAS along with far-infrared luminosities. Table 2 also contains blue and H α luminosities and HI masses.

2. Observations and Data Reduction

2.1. Infrared Space Observatory

On 1996 July 12, the ISO LWS observed the [C II] 158 μm line in the five sample galaxies. The [N II] 122 μm line was also observed in three of the galaxies. Details on these observations are given in Table 3. The observed positions are given in Table 1. To measure foreground Galactic emission at these locations, we also observed nearby (10' away)

²The National Radio Astronomy Observatory is operated by Associated Universities, Inc., under cooperative agreement with the National Science Foundation.

sky locations with the same observing parameters. These off-galaxy observations were concatenated onto the galaxy observations in a single observing sequence. The neighboring galaxies NGC 4189 and NGC 4222 shared a single sky measurement and were observed together in one concatenation chain, as were NGC 4294 and NGC 4299. We used the medium resolution grating mode, with a spectral scan width of 2 (2 spectral elements on either side of the line), giving a total of 5 resolution elements per scan, and a sampling interval of 4. The spectral resolution with this setup is $0.6 \mu\text{m}$, the total observed bandpass is $2.8 \mu\text{m}$, and the sampling interval is $0.14 \mu\text{m}$. At this resolution (1500 km s^{-1}), the lines are expected to be unresolved. The ‘fast’ scanning mode was used for these observations. The ISO LWS beam is FWHM $\sim 80''$ (Swinyard et al. 1996).

These data were processed by version 6.0 of the ISO pipeline, and were then further reduced (deleting bad data, summing scans) at the Infrared Processing and Analysis Center (IPAC) using version 1.2a of the Interactive Spectral Analysis Package (ISAP). The LWS version 6 pipeline includes a calibration correction based on internal illuminator flashes and a ‘drift’ correction for changing detector responsivities based on the source intensities. The absolute calibration uncertainties are expected to be less than 30%.

2.2. NRAO 12m Millimeter Telescope

The sample galaxies were observed in the CO (1 – 0) line on 1996 April 10-13, May 9-10, and December 14 and 20 with the 3 mm SIS receiver on the NRAO 12m telescope. At this frequency, the beamsize FWHM of the telescope is $55''$. Two 256×2 MHz filterbanks, one for each polarization, were used for these observations, providing a total bandpass of 1330 km s^{-1} and a spectral resolution of 5.2 km s^{-1} . The central velocity used for each galaxy is given in Table 1.

The positions observed with the 12m telescope are given in Table 5. For the two brightest galaxies, NGC 4189 and NGC 4522, we made a 5 point map with $25''$ spacing. For the fainter galaxies, we only observed the central point. Calibration was accomplished using an ambient chopper wheel. The observations were made using a nutating subreflector with a beam throw of $3'$ in the azimuthal direction. The pointing was checked periodically with bright continuum sources, and was consistent to $\sim 10''$. The CO spectra for each position were summed and a linear baseline subtracted.

3. Results

3.1. The ISO Data

The [C II] $158 \mu\text{m}$ spectra for the five galaxies are given in Figure 1 and the measured line fluxes are given in Table 4. All five sample galaxies were strongly detected in this line. The off positions show no line emission and significantly fainter continuum emission ($1 - 4 \times 10^{-20} \text{ W cm}^{-2} \mu\text{m}^{-1}$) than the galaxies. The [N II] $122 \mu\text{m}$ data for the three galaxies observed in this line are presented in Figure 2 and Table 4. Only NGC 4189 was detected in [N II]. As with [C II], the off positions show no [N II] emission and much weaker continuum emission (6 – 12 times fainter) than the galaxies.

3.2. CO (1 – 0) Data

The final CO spectra for the central positions in the galaxies are shown in Figure 1. In Table 5, we list the rms noise level T_R^* , the integrated CO flux densities $I_{CO} = \int T_R^* dV$, the peak temperature, and the FWZM line width for all of the observed positions. We detected four out of the five galaxies. In the Kenney & Young (1988) CO (1 – 0) study of these galaxies, only NGC 4189 was detected. When converted to the same units, our central flux

for this galaxy agrees with their value as tabulated in Young et al. (1995).

4. Discussion

4.1. Comparison with Other Galaxies

In Table 6, we list some derived parameters for these galaxies, including $M(H_2)$, assuming the standard Galactic I_{CO}/N_{H_2} ratio (Bloemen et al. 1986), $L([C\ II])$, $L([N\ II])$, $L(FIR)/M(H_2)$, and $L([C\ II])/L(CO)$. We also give a lower limit to the mass of hydrogen gas associated with the observed C^+ emission, $M_{C^+}^{min}(H) = 0.45\ L([C\ II])$, where $M_{C^+}^{min}(H)$ and $L([C\ II])$ are measured in solar units. This relationship is derived in the high density, high temperature limit ($n \gg 3000\ cm^{-3}$; $T \gg 91K$) as in Crawford et al. (1985), assuming solar carbon abundance and that all the C is in the form of C^+ ($[C^+]/[H] = 3 \times 10^{-4}$). For lower temperatures, densities, and abundances, higher masses are expected.

The $[C\ II]$ luminosities for these galaxies range from $5.7 \times 10^6\ L_\odot$ to $1.1 \times 10^7\ L_\odot$. Inspection of the IRAS HiRes images of these galaxies indicate that they are essentially unresolved in the $85'' \times 50''\ 60\ \mu m$ HiRes beam, so nearly all the far-infrared flux originates within the ISO beam. The global $L([C\ II])/L(FIR)$ ratios for these galaxies therefore range from 0.004 – 0.008. For comparison, the galaxies surveyed by Stacey et al. (1991) have $L([C\ II])/L(FIR)$ ratios between 0.0015 – 0.006, while in the Galactic plane $L([C\ II])/L(FIR) \sim 0.006$ (Nakagawa et al. 1995). In the LMC $L([C\ II])/L(FIR)$ is slightly higher, $\sim 1\%$ (Mochizuki et al. 1994; Israel et al. 1996). Global flux ratios for the spiral galaxies NGC 6946 (Madden et al. 1993) and NGC 5713 (Lord et al. 1996) are ~ 0.011 and 0.007, respectively. Thus the $L([C\ II])/L(FIR)$ ratios in the surveyed Virgo galaxies are not unusual compared to other galaxies.

In contrast to $L([C\ II])/L(FIR)$, the $L([C\ II])/L(CO)$ ratios for the sample galaxies

vary widely, ranging from 1650 in NGC 4189 to 15,600 in NGC 4299. This variation is evident in Figure 1, where the CO and [C II] spectra are plotted together. These differences are too large to be accounted for by the calibration uncertainties alone. The highest values of $L([C II])/L(CO)$ are typical of the global ratio found for the LMC, $\sim 23,000$ (Mochizuki et al. 1994), but are not as high as at selected HII regions within the LMC, for example, at 30 Dor, where the ratio is $\sim 70,000$ (Poglitsch et al. 1995). The $L([C II])/L(CO)$ ratios for NGC 4294 and NGC 4299 are higher than those typically found in the central regions of high mass galaxies, ~ 4000 in starbursts and ~ 1300 in quiescent galaxies (Stacey et al. 1991). In the disk of the Milky Way, $L([C II])/L(CO) \sim 1300$ (Nakagawa et al. 1995).

The observed $L([N II]) 122 \mu m/L([C II])$ ratios are 0.078 for NGC 4189 and ≤ 0.058 and ≤ 0.069 for NGC 4294 and NGC 4299, respectively. For comparison, this ratio is 0.2 in the starburst galaxy M82 (Petuchowski et al. 1994), 0.08 – 0.1 in the Milky Way (Bennett et al. 1994; Bennett 1996), ≤ 0.18 in the merging pair NGC 4038/9 (Fischer et al. 1996), and ≤ 0.12 in the spiral galaxy NGC 5713 (Lord et al. 1996). Thus the high $L([C II])/L(CO)$ galaxies appear somewhat weak in [N II] compared to more massive galaxies, although the paucity of available extragalactic [N II] detections and the ISO calibration errors makes this result uncertain.

In the two galaxies with the highest $L([C II])/L(CO)$ ratios, NGC 4294 and NGC 4299, the $L(FIR)/M(H_2)$ ratios are more than 8 times larger than the mean value found for the higher mass Virgo galaxies in Kenney & Young (1988). Thus two out of the five galaxies in this sample appear to be extreme in comparison to higher mass galaxies, with significantly higher $L([C II])/L(CO)$ and $L(FIR)/M(H_2)$ values but low $L([N II]) 122 \mu m/L([C II])$ ratios. $L(B)/L(CO)$ is also enhanced in NGC 4294 and NGC 4299 relative to the other galaxies in the sample. In contrast, the $L([C II])/L(FIR)$ ratio is only marginally higher in NGC 4294 and NGC 4299.

4.2. PDRs and Metallicity

In the central regions of high mass spiral galaxies, the $L([\text{C II}])/L(\text{FIR})$ and $L([\text{C II}])/L(\text{CO})$ ratios are consistent with theoretical models of emission from PDRs with solar abundances (Crawford et al. 1985; Stacey et al. 1991). As noted previously, three of the galaxies in our Virgo sample, NGC 4189, NGC 4222, and NGC 4522, have $L([\text{C II}])/L(\text{FIR})$ and $L([\text{C II}])/L(\text{CO})$ ratios similar to those seen in high mass galaxies, indicating that solar metallicity PDRs can also account for the $[\text{C II}]$ emission from these galaxies.

Two of our galaxies, however, have extreme $L([\text{C II}])/L(\text{CO})$ values, more similar to those found for low metallicity dwarfs than for high mass spirals. In general, their CO fluxes are very weak relative to their far-infrared, blue, and $[\text{C II}]$ fluxes, suggesting that the difference between these galaxies and the other three galaxies may be due to a deficiency in CO rather than an excess in $[\text{C II}]$.

The similarity with dwarf galaxies suggests that low metallicity and therefore a low $I_{\text{CO}}/N_{\text{H}_2}$ ratio may be responsible. In dwarf galaxies, enhanced $L([\text{C II}])/L(\text{CO})$ ratios are explained by low dust and metal content (Mochizuki et al. 1994; Poglitsch et al. 1995; Israel et al. 1996; Madden et al. 1997). Although no measurements of metallicity are available for these Virgo spirals at present, they have relatively low blue luminosities which suggests they may be metal-poor. Their absolute blue magnitudes, ~ -18 to -19 , are similar to that of the LMC and other dwarf galaxies which are known to be metal-poor (Skillman, Kennicutt, & Hodge 1989). Less than solar metallicities have also been seen in spiral and starburst galaxies at these magnitudes (Vila-Costas & Edmunds 1992; Storch-Bergmann, Calzetti, & Kinney 1994).

If metallicity is responsible, though, it is surprising that NGC 4294 and NGC 4299 are weak in CO while the other three galaxies are not, since all five galaxies have approximately

the same apparent blue magnitudes (Table 1). The far-infrared flux densities are also similar (Table 2). Variations in the $L([\text{C II}])/L(\text{CO})$ ratio could be caused by the smaller CO beam missing emission contained in the larger ISO beam, however, $\text{H}\alpha$ images of these galaxies (Hodge & Kennicutt 1983) show that most of the star formation is occurring within the inner arcminute, suggesting that most of the CO in these galaxies is contained in the central beam.

A possible explanation for the more extreme $L([\text{C II}])/L(\text{CO})$ values for NGC 4294 and NGC 4299 is that they may be closer, and therefore have lower blue luminosities and masses than the other three galaxies. The Virgo Cluster has long been known to have a complicated morphology (c.f., Binggeli, Tammann, & Sandage 1987; Pierce & Tully 1988), and may have considerable extent along the line of sight. A recent Tully-Fisher study derives distances for individual galaxies in the Virgo Cluster ranging from 12 to 30 Mpc (Yasuda, Fukugita, & Okamura 1997). For NGC 4294, they quote a distance of only 13.6 ± 1.1 Mpc, while NGC 4189, NGC 4222, and NGC 4522 were found to be more distant, at 33.8 ± 5.1 Mpc, 22.9 ± 1.5 Mpc, and 16.3 ± 1.1 Mpc, respectively. No Tully-Fisher distance was derived for the face-on galaxy NGC 4299, however, it may be in a bound pair with NGC 4294, which is only a few radii away on the sky. The optical and HI morphologies and HI kinematics of this pair are disturbed, suggesting a recent interaction (Sandage, Binggeli, & Tammann 1985; Warmels 1988a). If NGC 4294 and NGC 4299 have lower blue luminosities and masses than the other three galaxies then they may have lower metallicities as well, which could explain the enhanced $L([\text{C II}])/L(\text{CO})$ values.

There may also be a spread in metallicity among these galaxies, even if they have similar blue luminosities. In the van den Bergh & Pierce (1990) study of dust in Virgo cluster galaxies, NGC 4189, NGC 4222, and NGC 4522 are all classed as dusty or very dusty. They do not fit the average magnitude-dustiness relationship for Virgo galaxies,

being dustier than expected (van den Bergh & Pierce 1990). This suggests that they may be more metal-rich than typical for their magnitudes. Alternatively, an interaction between NGC 4294 and NGC 4299 may have driven unprocessed gas into the centers of these galaxies, causing the inner regions of these galaxies to have significantly lower metallicities than other galaxies of similar mass. This question of metallicity should be tested with followup optical spectroscopy.

Another possible explanation for the differences between the galaxies is that they are in different evolutionary stages. Perhaps NGC 4294 and NGC 4299 are in a post-burst stage where the molecular gas has been depleted but PDR [C II] emission is still bright. Within the Large Magellanic Cloud, the wide variation in the observed $L([C II])/L(CO)$ ratio has been attributed to evolutionary differences (Israel et al. 1996). NGC 4294 and NGC 4299 have somewhat higher $H\alpha$ fluxes than the other three galaxies (Table 2), and therefore more star formation activity, if they are all at the same distance. Their $H\alpha$ equivalent widths are among the highest in the Kennicutt & Kent (1983) galaxy sample, similar to those of starburst galaxies, thus they have a high current to past star formation rate. The optical photographs of NGC 4294 and NGC 4299 presented in Sandage et al. (1985) show disturbed spiral structure containing numerous bright HII regions. NGC 4294 and NGC 4299 also have higher 60 μm to 100 μm flux ratios than the other three galaxies (Table 2), indicating warmer dust. Thus strong ultraviolet radiation fields may contribute to the enhanced $L([C II])/L(CO)$ ratios in these galaxies. However, the observed ratios are much more extreme than those typically seen in starburst galaxies (Stacey et al. 1991), indicating that star formation and gas depletion are probably not solely responsible for the observed line ratios.

4.3. Emission from Diffuse HI Clouds

An alternative explanation for the enhanced $L([\text{C II}])/L(\text{CO})$ ratios in NGC 4294 and NGC 4299 is that there is a large component of C^+ associated with diffuse atomic gas. Spatially resolved $[\text{C II}]$ observations of the nearby spiral galaxy NGC 6946 (Madden et al. 1993) revealed a very extended component containing $\sim 70\%$ of the total $[\text{C II}]$ emission of the galaxy. This diffuse emission is thought to be due to C^+ arising from diffuse HI clouds rather than standard PDRs. If emission from diffuse atomic gas rather than PDRs dominates in these galaxies, then one would not expect a strong correlation between CO and $[\text{C II}]$ fluxes.

At Virgo, the ISO beam covers an area 3.9 kpc in radius, assuming a distance of 20 Mpc. Extended $[\text{C II}]$ radiation is seen at this radius in NGC 6946 (Madden et al. 1993). Optical images of the Virgo galaxies (Sandage et al. 1985) show that the ISO beam covers not just the nuclei but also most of the observed spiral arms, so may contain considerable diffuse disk emission. The spread in $L([\text{C II}])/M(\text{HI})$ for the sample galaxies is only a factor of 3, compared to a factor of 20 in $L([\text{C II}])/L(\text{CO})$. Thus the observed $[\text{C II}]$ fluxes are more closely correlated with the total HI mass than with CO.

To compare the observed $[\text{C II}]$ and HI fluxes for these galaxies more accurately, it is first necessary to take into account the fact that the observed HI distributions extend beyond the ISO beam. Four out of the 5 galaxies in our sample have published interferometric HI maps (Warmels 1988a; Cayette et al. 1990) in which HI is detected out to radii of $\sim 2'$. Over the ISO beam, the column density of HI is $\sim 10^{21} \text{ cm}^{-2}$ in NGC 4189, NGC 4294, and NGC 4299, and a factor of ~ 3 times lower in NGC 4222 (Warmels 1988b). The fraction of the total HI contained within an $\sim 80''\text{--}90''$ diameter in these galaxies is $35\% \sim 64\%$ (Warmels 1988b), so $4 - 8 \times 10^8 M_\odot$ of atomic hydrogen is contained within the ISO beam. Thus our galaxies have $M(\text{HI})/L([\text{C II}]) = 40 - 90 M_\odot/L_\odot$ within the ISO

beam. For comparison, the extended [C II] emission in NGC 6946 has $M(\text{HI})/L([\text{C II}]) \sim 16 M_{\odot}/L_{\odot}$ (Madden et al. 1993). Thus the amount of HI gas relative to the [C II] flux is even higher in our sample galaxies than in the outer disk of NGC 6946.

These galaxies are relatively rich in HI. In NGC 4294 and NGC 4299 in particular the interstellar medium may be predominantly atomic if CO is not greatly underestimating the molecular gas; the Galactic $I_{\text{CO}}/N_{\text{H}_2}$ ratio gives $M(\text{HI})/M(\text{H}_2)$ ratios of ≥ 20 for these galaxies. We note that in spite of the fact that these galaxies are in the Virgo Cluster they are not extremely HI-deficient for their types; their HI contents, defined according to the scale in Giovanelli & Haynes (1983), are fairly typical of field galaxies (Kenney & Young 1988). Only NGC 4522 appears somewhat HI deficient (Kenney & Young 1988). The five sample galaxies lie in the outer regions of the Virgo Cluster, at cluster radii of $2.5 - 4.5$, and so are not subject to as strong HI removal mechanisms as galaxies in the cluster core.

As in the Milky Way (Kulkarni & Heiles 1987), the atomic gas in external galaxies may exist in two forms: cold HI clouds (cold neutral medium; $\sim 80\text{K}$) and warm diffuse HI (warm neutral medium; $\sim 6000\text{K}$). To estimate the amount of [C II] arising from cold atomic clouds in our sample galaxies, we use the relationship $M(\text{HI})/L([\text{C II}]) = [580/(n_{\text{H}}e^{-91/T})][3 \times 10^{-4}/X_{\text{C}^+}]$, where the mass of HI and luminosity of [C II] are in solar units, n_{H} is the density of H atoms in cm^{-3} , T is the kinetic temperature of the gas in degrees K, and X_{C^+} is the abundance $[\text{C}^+]/[\text{H}]$. This formula was derived from the relationship for collisional excitation of the C^+ line in the optically thin case (Crawford et al. 1985), in the low density ($n \ll 4 \times 10^3 \text{ cm}^{-3}$) limit. For cold HI clouds, collisional excitation by electrons should not be important (Crawford et al. 1985; Madden et al. 1993). Assuming a solar abundance $[\text{C}^+]/[\text{H}] = 3 \times 10^{-4}$ and typical values of T and n_{H} for the cold neutral medium of 80K and 90 cm^{-3} (Kulkarni & Heiles 1987; Madden et al. 1993) gives an expected ratio of $M(\text{HI})/L([\text{C II}]) = 20 M_{\odot}/L_{\odot}$.

We therefore conclude that, if CNM with $T \sim 80\text{K}$ and $n_H \sim 90 \text{ cm}^{-3}$ makes up $\sim 50\%$ of the observed HI in these galaxies, there are sufficient cold atomic clouds in these galaxies to account for all of the observed C^+ emission. If the atomic gas is colder and more diffuse, however, or if the fraction of HI emission originating from the CNM is lower, then only a fraction of the C^+ can be accounted for by the CNM. Likewise, if the metallicity is low, all of the $[\text{C II}]$ emission cannot arise from the CNM.

The WNM, in contrast to the CNM, does not appear to be a major contributor to the observed $[\text{C II}]$ flux from our galaxies. Unlike in the CNM, in the WNM C^+ excitation by electrons is an important factor (Madden et al. 1993). Including this term as in equation 5 of Madden et al. (1993), and including the critical density terms for collisions with HI and electrons as in Launay & Roueff (1977) and Hayes & Nussbaumer (1984), for the WNM the relationship between temperature, hydrogen density, and HI and $[\text{C II}]$ emission is: $L([\text{C II}])/M(\text{HI}) = [3 \times 10^{-4}/X_{\text{C}^+}] [2/(1 + 710/n_H) + 2/(1 + 0.13T^{1/2}/(X_e n_H))]$, where $M(\text{HI})$ and $L([\text{C II}])$ are in solar units, T is in degrees K, n_H is in cm^{-3} , X_e is the fractional ionization of hydrogen, and X_{C^+} is the C^+ abundance. Assuming solar abundance and the Galactic WNM parameters of $X_e = 0.03$, $T = 6000\text{K}$, and $n \sim 1 \text{ cm}^{-3}$ (Kulkarni & Heiles 1987) gives a predicted relationship between HI mass and $[\text{C II}]$ luminosity of $M(\text{HI})/L([\text{C II}]) \sim 120 M_\odot/L_\odot$. This is higher than the observed ratios in the Virgo galaxies, indicating that there is not sufficient WNM in these galaxies to account for the observed $[\text{C II}]$ emission. This same conclusion was reached for the extended emission in the more massive spiral galaxy NGC 6946 (Madden et al. 1993).

4.4. Ionized Gas

$[\text{C II}]$ emission may also originate from HII regions, both compact and diffuse. HII regions with densities from $10^2 - 10^5 \text{ cm}^{-3}$ have been modeled in detail by Rubin (1985).

These models provide expected $L(\text{H}\alpha)/L([\text{C II}])$ ratios for HII regions ionized by stars with temperatures ranging from 31,000K – 45,000K. For solar abundance and a Lyman continuum photon rate of 10^{49} photons s^{-1} , this ratio ranges from 9.8 – 16.1 for a density of 100 cm^{-3} and a central star temperature between 31,000K and 37,000K. This ratio increases rapidly with density and stellar temperature, to 1.4×10^5 for a density of 10^5 cm^{-3} and a stellar temperature of 40,000K, because of an increased fraction of doubly ionized carbon. Higher stellar luminosities and lower abundances give even higher ratios.

These models can be compared with the observed values for these galaxies, after correcting the $\text{H}\alpha$ fluxes for extinction and contributions from diffuse gas. For NGC 4294 and NGC 4299, we estimate average extinctions of $A_V \sim 0.5$ over the ISO beam, using the HI column densities from Warmels (1988b) and the standard Galactic relationship between hydrogen column density and extinction from Bohlin, Savage, & Drake (1978), assuming molecular gas is negligible (i.e., assuming the standard Galactic $I_{\text{CO}}/N_{\text{H}_2}$ ratio). We assume $\sim 35\%$ of the observed $\text{H}\alpha$ emission from these Virgo galaxies comes from the diffuse ionized gas (warm ionized medium; WIM), as in M31, the Magellanic Clouds, and other nearby spiral galaxies (Walterbos & Braun 1994; Kennicutt et al. 1995; Hoopes, Walterbos, & Greenawalt 1996). This calculation indicates that 10 – 20% of the total observed $[\text{C II}]$ emission from these galaxies may arise from classical HII regions, if the ionizing stars have temperatures between 31,000K and 37,000K, the HII region densities are $\sim 100 \text{ cm}^{-3}$, and the abundances are solar. For higher stellar temperatures and gas densities or lower abundances, this fraction decreases. On the other hand, if the extinction is underestimated, HII regions may contribute a larger portion of the observed $[\text{C II}]$ flux.

Rubin (1985) does not model low density HII regions, so we estimate their contributions via the relationship $M(\text{HII})/L([\text{C II}]) = [0.5 + T^{1/2}/(15X_{\text{enH}})] (3 \times 10^{-4}/X_{\text{C}+})$. In this formula, $M(\text{HII})$ and $L([\text{C II}])$ are in solar units, T is in degrees K, and n_{H} is in cm^{-3} .

This equation was derived from the above relationship for the WNM, using the fact that in ionized gas, excitation is dominated by collisions with electrons. Using solar abundances and typical values for the WIM in the Milky Way of 8000K, $n_H \sim 0.5 \text{ cm}^{-3}$, and $X_e \geq 0.75$ (Kulkarni & Heiles 1987), the ratio $M(\text{HII})/L([\text{C II}]) \sim 15 \text{ M}_\odot/\text{L}_\odot$.

The mass of diffuse ionized hydrogen in these galaxies can be estimated from their extinction-corrected $\text{H}\alpha$ luminosities. Using the case B 10,000K relationship (Osterbrock 1989), $L(\text{H}\alpha) \sim 0.11 M(\text{HII}) n_H$, where $L(\text{H}\alpha)$ is in L_\odot , $M(\text{HII})$ is in M_\odot , and n_H is in cm^{-3} . For the WIM, where $n_H \sim 0.5 \text{ cm}^{-3}$, $L(\text{H}\alpha) \sim 0.55 M(\text{HII})$. Assuming 35% of the observed $\text{H}\alpha$ emission comes from the WIM, we estimate that the HII mass in the WIM is $\sim 2.4 \times 10^7 \text{ M}_\odot$ in these galaxies. The expected $[\text{C II}]$ luminosity is therefore $1.6 \times 10^6 \text{ L}_\odot$ for the WIM.

We therefore conclude that ionized hydrogen regions contribute $\leq 35\%$ of the total observed $[\text{C II}]$ emission from these galaxies, with roughly 15% originating in the WIM and $\leq 20\%$ in standard HII regions. These percentages are uncertain because the extinction is poorly determined, as is the density and the ratio of diffuse to dense HII mass. Multi-frequency high spatial resolution radio continuum observations and deep $\text{H}\alpha$ imaging of these galaxies would be helpful in better determining the contributions from these components to the observed $[\text{C II}]$ emission.

As noted previously, NGC 4294 and NGC 4299 may have relatively low $L([\text{N II}])/L([\text{C II}])$ ratios compared to the starburst galaxy M82. Since the ionization energy of nitrogen is less than that of hydrogen and $[\text{N II}]$ is only found in HII regions, these low $L([\text{N II}])/L([\text{C II}])$ ratios suggest that C^+ associated with ionized hydrogen may be less important in NGC 4294 and NGC 4299 than in starburst galaxies such as M82. This result is quite uncertain, however, because of the calibration uncertainties and the lack of published $[\text{N II}]$ measurements for the WIM. This analysis emphasizes the need for spatially

resolved far-infrared line studies of nearby galaxies, such as the Madden et al. (1993) study, to better distinguish the various components of [C II] emission.

5. Conclusions

We have observed the [C II] 158 μm , [N II] 122 μm , and CO (1 – 0) emission from five Virgo spiral galaxies with low blue luminosity. In three of the sample galaxies, the observed fluxes are consistent with emission from solar metallicity PDRs. In two out of the five galaxies in the sample, however, we find high $L([\text{C II}])/L(\text{CO})$ and $L(\text{FIR})/L(\text{CO})$ ratios, more typical of dwarf irregular galaxies than of high mass spirals. These enhanced ratios may be caused by low metallicities, and therefore non-Galactic $I_{\text{CO}}/N_{\text{H}_2}$ ratios. Alternatively, C^+ emission from cold neutral HI clouds rather than PDRs may dominate the [C II] emission in these galaxies, or both HI-dominated regions and low metallicity PDRs may contribute to the observed [C II] emission. The WIM and standard HII regions contribute less than a third of the observed [C II] emission.

We are grateful to the entire ISO team for all their hard work on ISO. We particularly thank the LWS instrument team and the Vilspa ground support, as well as the ISO staff at the Infrared Processing and Analysis Center (IPAC). We also thank Jeff Kenney, Steve Lord, Phil Maloney, and an anonymous referee for helpful comments on the manuscript. We appreciate the help of the NRAO staff in making the CO observations, particularly the telescope operators Lisa Engel, Paul Hart, Mark Metcalf, and Victor Gasho. This research has made use of the NASA/IPAC Extragalactic Database (NED) which is operated by the Jet Propulsion Laboratory, Caltech, under contract with the National Aeronautics and Space Administration. A portion of this work was performed while B.J.S. held a National Research Council Research Associateship at the Jet Propulsion Laboratory. This work was

supported in part by ISO data analysis funding from the US National Aeronautics and Space Administration.

REFERENCES

- Bennett, C. L., et al. 1994, *ApJ*, 434, 587
- Bennett, C. L., 1996, private communication
- Binggeli, B., Tammann, G. A., & Sandage, A. 1987, *AJ*, 94, 251
- Bloemen, J. B. G. L. et al. 1986, *A&A*, 154, 25
- Bohlin, R. C., Savage, B. D., & Drake, J. F. 1978, *ApJ*, 224, 132
- Cayette, V., van Gorkom, J. H., Balkowski, C., & Kotanyi, C. 1990, 100, 604
- Clegg, P. E., et al. 1996, *A&A*, 315, L38
- Combes, F. 1986, in *Star Forming Dwarf Galaxies and Related Objects*, eds. D. Kunth, T. X. Thuan, & J. Tran Thanh Van (Singapore: Kim Hup Lee Printing Co.), 307
- Crawford, M. K., Genzel, R., Townes, C. H., & Watson, D. M. 1985, *ApJ*, 291, 755
- Dettmar, R.-J., & Heithansen, A. 1989, *ApJ*, 344, L61
- De Vaucouleurs, G., De Vaucouleurs, A., Corwin Jr., H.G., Buta, R. J., Paturel, G., & Fouque, P. 1991, *Third Reference Catalogue of Bright Galaxies, Version 3.9 (RC3)*
- Fischer, J., et al. 1996, *A&A*, 315, L97
- Garnett, D. R., & Shields, G. A. 1987, *ApJ*, 317, 82
- Giovanelli, R., & Haynes, M. P. 1983, *AJ*, 88, 881
- Haynes, M. A., & Nussbaumer, H. 1984, *A&A*, 134, 193
- Helou, G., Khan, I. R., Malek, L., & Boehmer, L. 1988, *ApJS*, 68, 151
- Hodge, P. W., & Kennicutt, R. C. 1983, *AJ*, 88, 296
- Hoopes, C. G., Walterbos, R. A. M., & Greenawalt, B. E. *AJ*, 112, 1429

- Israel, F. P., Maloney, P. R., Geis, N., Herrmann, F., Madden, S. C., Poglitsch, A., & Stacey, G. J. 1996, *ApJ*, 465, 738
- Kenney, J. D., & Young, J. S. 1988, *ApJ*, 326, 588
- Kenney, J. D., & Young, J. S. 1989, *ApJ*, 344, 171
- Kennicutt, R. C., Jr., Bresolin, R., Bomans, D. J., Bothun, G. D., & Thompson, I. B. 1995, *AJ*, 109, 594
- Kennicutt, R. C., & Kent, S. M. 1983, *AJ*, 88, 1094
- Kessler, M., et al. 1996, *A&A*, 315, L27
- Koopmann, R. A., Kenney, J. D. P., & Young, J. S. 1997, in preparation
- Kulkarni, S., & Heiles, C. 1987, in *Interstellar Processes*, ed. D. J. Hollenbach & H. A. Thronson (Dordrecht: Reidel), 87
- Launay, J. M., & Roueff, E. 1977, *J. Phys. B.*, 10, 879
- Lord, S. D., et al. 1996, *A&A*, 315, L117
- Madden, S. C., Geis, N., Genzel, R., Herrmann, F., Jackson, J., Poglitsch, A., Stacey, G. J., & Townes, C. H. 1993, *ApJ*, 407, 579
- Madden, S. C. et al. 1997, in press
- Maloney, P. 1990, *The Interstellar Medium in Galaxies*, ed. H. Thronson & M. Shull (Boston: Kluwer Academic Press), 493
- Maloney, P., & Wolfire, M. G. 1996, *IAU Symposium 170: CO: Twenty-Five Years of Millimeter-Wave Spectroscopy*, (Tucson, AZ), in press.
- Maloney, P., & Black, J. H. 1988, *ApJ*, 325, 389
- Mangum, J. G. 1997, *User's Manual for the NRAO 12m Millimeter-Wave Telescope* (NRAO: Tucson).

- Mochizuki, K. et al. 1994, ApJ, 430, L37
- Nakagawa, T., Doi, Y., Yui, Y. Y., Okuda, H., Mochizuki, K., Shibai, H., Nishimura, T., & Low, F. J. 1995, ApJ, 455, L35
- Ohta, K. et al. 1993, PASJ, 45, L21
- Osterbrock, D. E. 1989, *Astrophysics of Gaseous Nebulae and Active Galactic Nuclei* (Mill Valley, CA: University Science Books).
- Pagel, B. E. J., & Edmunds, M. G. 1981, ARA&A, 19, 77
- Pierce, M. J. & Tully, R. B. 1988, ApJ, 330, 579
- Poglitsch, A., Krabbe, A., Madden, S. C., Nikola, T., Geis, N., Johansson, L. E. B., Stacey, G. J., & Sternberg, A. 1995, ApJ, 454, 293
- Rubin, R. H. 1985, ApJS, 57, 349
- Rubio, M., Garay, G., Montani, J., & Thaddeus, P. 1991, ApJ, 368, 173
- Sandage, A., Binggeli, B., & Tammann, G. A. 1985, AJ, 90, 395
- Sandage, A., & Tammann, G. A. 1981, *A Revised Shapley-Ames Catalog of Bright Galaxies* (Washington D.C.: Carnegie Institution of Washington)
- Skillman, E. D., Kennicutt, R. C., & Hodge, P. W. 1989, ApJ, 347, 875
- Stacey, G. J., Geis, N., Genzel, R., Lugten, J. B., Poglitsch, A., Sternberg, A., & Townes, C. H. 1991, ApJ, 373, 423
- Storchi-Bergmann, T., Calzetti, D., & Kinney, A. L. 1994, ApJ, 429, 572
- Swinyard, B. M., et al. 1996, A&A, 315, L43
- Tacconi, L. J., & Young, J. S. 1987, ApJ, 322, 681
- Tielens, A., & Hollenbach, D. 1985, ApJ, 291, 722
- van den Bergh, S., & Pierce, M. J. 1990, ApJ, 364, 444

- Vila-Costas, M. B., & Edmunds, M. G. 1992, MNRAS, 259, 121
- Walterbos, R. A. M., & Braun, R. 1994, ApJ, 431, 156
- Warmels, R. H. 1988a, A&AS, 72, 19
- Warmels, R. H. 1988b, A&AS, 72, 427
- Wilson, C. D., & Reid, I. N. 1991, ApJ, 366, L11
- Wolfire, M., Hollenbach, D., & Tielens, A. 1989, ApJ, 344, 770
- Yasuda, N., Fukugita, M., & Okamura, S. 1997, ApJS, 108, 417
- Young, J. S. 1990, The Interstellar Medium in Galaxies, ed. H. Thronson & M. Shull
(Boston: Kluwer Academic Press), 67
- Young, J. S., & Scoville, N. Z. 1991, ARA&A, 29, 581
- Young, J. S., et al. 1995, ApJS, 98, 219

CAPTIONS

Fig. 1.— Left column: the final summed CO (1 – 0) spectra for the central positions in the sample galaxies. Note that these plots all have the same y-axis scale. Right column: the final [C II] 158 μm spectra for the sample galaxies. These data are all plotted with the same y-axis scale.

Fig. 2.— Figure 2. The final [N II] 122 μm spectra for the three observed galaxies.

Table 1
Program Galaxies

Galaxy	Type ¹	Type ²	R.A. (1950)			Dec. ³ (1950)			B _T ^{0,1}	D ₂₅ ¹ (')	velocity ¹ (km/s)
NGC 4189	ScII.2	SBc(sr)II.2	12	11	14.5	13	42	11	12.2	2.4	2113
NGC 4222	Sd	—	12	13	50.1	13	35	8	12.7	3.3	226
NGC 4294	ScII-III	SBc(s)II-III	12	18	45.3	11	47	10	11.8	3.2	355
NGC 4299	ScdIII	Sd(s)III	12	19	7.7	11	46	48	12.7	1.7	232
NGC 4522	SBcd	Sc/Sb	12	31	7.6	9	27	3	12.0	3.7	2324

¹From de Vaucouleurs et al. 1993 (RC3). The velocities are heliocentric.

²From Sandage & Tammann (1981).

³The positions are from the NASA Extragalactic Database (NED).

Table 2
Parameters of Sample Galaxies

Galaxy	F(60) ¹ (Jy)	F(100) ¹ (Jy)	L(FIR) ² (L _⊙)	L(B) ³ (L _⊙)	L(Hα) ⁴ (L _⊙)	M(HI) ⁵ (M _⊙)
NGC 4189	3.6	9.1	2.7×10^9	8.3×10^9	1.4×10^7	1.2×10^9
NGC 4222	1.1	3.3	9.0×10^8	5.2×10^9	—	1.6×10^9
NGC 4294	3.0	5.5	1.9×10^9	1.2×10^{10}	2.0×10^7	2.2×10^9
NGC 4299	2.7	4.7	1.7×10^9	5.2×10^9	2.5×10^7	1.2×10^9
NGC 4522	1.6	4.7	1.3×10^9	1.0×10^{10}	5.3×10^6	6×10^8

All values calculated assuming D = 20 Mpc for the Virgo Cluster.

¹The far-infrared flux densities are from the IRAS satellite using the AddScan program.

² $L(\text{FIR}) = 3.65 \times 10^5 (2.58 F(60) + F(100))D^2$, where F(60) and F(100) are in Jy, D is in Mpc, and L(FIR) in L_⊙ (Helou et al. 1988).

³Using $M_B(\odot) = 5.48$.

⁴From Koopmann, Kenney, & Young 1997, uncorrected for extinction.

⁵Total HI mass, from Kenney & Young 1988.

Table 3
Observing Parameters for ISO

Galaxy	Wavelength (μm)	Time/Step ^a (seconds)	Number ^a Scans
NGC 4189	158.86	1.2	3
	122.76	32.0	80
NGC 4222	157.86	8.4	21
NGC 4222 OFF	157.86	8.4	21
	122.76	32.0	80
NGC 4294	158.93	2.4	6
	122.04	24.0	60
NGC 4299	157.86	2.8	7
	121.99	24.0	60
NGC 4299 OFF	157.86	2.8	7
	121.99	24.0	60
NGC 4522	158.96	5.2	13
NGC 4522 OFF	158.96	5.2	13

^aThe integration time per step (wavelength position) per scan is 0.4 seconds.

Table 4
Far-Infrared Line Fluxes for Sample Galaxies

Galaxy	Line (μm)	Flux ^a (W m^{-2})
NGC 4189	[C II] 158 μm	$9.1 \pm 0.8 \times 10^{-16}$
	[N II] 122 μm	$6.9 \pm 0.7 \times 10^{-17}$
NGC 4222	[C II] 158 μm	$4.5 \pm 0.9 \times 10^{-16}$
NGC 4294	[C II] 158 μm	$8.4 \pm 0.9 \times 10^{-16}$
	[N II] 122 μm	$\leq 5.1 \times 10^{-17}$
NGC 4299	[C II] 158 μm	$6.8 \pm 0.9 \times 10^{-16}$
	[N II] 122 μm	$\leq 4.7 \times 10^{-17}$
NGC 4522	[C II] 158 μm	$8.1 \pm 0.9 \times 10^{-16}$

^aThe quoted uncertainties are statistical; they do not include the calibration uncertainty.

Table 5
CO (1-0) Results for Sample Galaxies

Galaxy	ID	Position Observed						I_{CO}^a	T_R^* (rms) ^b	ΔV^c
		R.A. (1950)		Dec. (1950)				(K km s ⁻¹)	(mK)	(km s ⁻¹)
NGC 4189	C	12	11	14.5	13	42	11.0	3.95 ± 0.37	7.0	550
	E	12	11	16.2	13	42	13.0	2.87 ± 0.31	8.1	290
	W	12	11	12.8	13	42	9.0	1.80 ± 0.19	8.0	110
	N	12	11	14.4	13	42	36.0	1.89 ± 0.37	7.9	420
	S	12	11	14.7	13	41	46.0	3.38 ± 0.31	6.7	420
NGC 4222	C	12	13	50.1	13	35	8.0	0.73 ± 0.14	3.6	300
NGC 4294	C	12	18	45.3	11	47	10.0	—	3.3	—
NGC 4299	C	12	19	7.7	1	46	48.0	0.28 ± 0.05	2.2	100
NGC 4522	C	12	31	7.6	9	27	3.0	4.33 ± 0.34	6.6	520
	E	12	31	9.0	9	27	17.0	0.63 ± 0.44	10.9	310
	W	12	31	6.2	9	26	49.0	2.35 ± 0.46	11.5	420
	N	12	31	8.8	9	27	24.0	2.54 ± 0.43	8.3	520
	S	12	31	6.7	9	26	42.0	0.87 ± 0.40	9.2	360

^a $I_{CO} = \int T_R^* dv$. For the 12m telescope at 115 GHz, the conversions from T_R^* to antenna temperature T_A^* and main beam temperature T_{MB} are $T_A^* = 0.68 T_R^*$ and $T_{MB} = T_R^*/0.82$ (Mangum 1997).

^brms value in a 5.2 km/s channel.

^cFull width zero maximum (FWZM).

Table 6
Derived Parameters for Virgo Galaxies^a

Galaxy	$M(H_2)^b$ (M_\odot)	$L([C\ II])$ (L_\odot)	$L([N\ II])$ (L_\odot)	$\frac{L(FIR)}{M(H_2)}$ (L_\odot/M_\odot)	$\frac{L([C\ II])}{L(CO)}^c$	$M_{C^+}^{min}(H)^d$ (M_\odot)
NGC 4189	6.6×10^8	1.1×10^7	8.6×10^5	4.1	1650	5.0×10^6
NGC 4222	1.3×10^8	5.7×10^6	—	6.9	3960	2.6×10^6
NGC 4294	$\leq 7.1 \times 10^7$	1.1×10^7	$\leq 6.4 \times 10^5$	≥ 27	$\geq 14,300$	4.8×10^6
NGC 4299	5.1×10^7	8.6×10^6	$\leq 5.9 \times 10^5$	33	15,600	3.9×10^6
NGC 4522	5.0×10^8	1.0×10^7	—	2.6	1840	4.6×10^6

^aMasses and luminosities calculated assuming a distance of 20 Mpc to the Virgo Cluster.

^bAssuming the standard Galactic I_{CO}/N_{H_2} ratio (Bloemen et al. 1986) and 34 Jy/K. For the galaxies where only one position was measured, we assumed the source fills the beam ($\eta_c = 0.82$). For the other two galaxies, we assumed an intrinsic Gaussian distribution. The upper limit for NGC 4294 is 3σ assuming a line width of 300 km/s (FWZM HI line width; Warmels 1988a).

^c $L(CO)$ derived using $L(CO) = 0.119 D^2 S_{CO}$ (Kenney & Young 1989), where D is the distance in Mpc and S_{CO} is the CO flux in Jy km s⁻¹.

^dMinimum mass of hydrogen associated with C⁺ emission, as described in the text.